

To appear in The Astronomical Journal

The Lithium Rotation Correlation in the Pleiades Revisited

Jeremy R. King

Department of Physics, University of Nevada, Las Vegas¹, 4505 S. Maryland Parkway, Las Vegas, NV 89154-4002

and

Space Telescope Science Institute, 3700 San Martin Drive, Baltimore, MD 21218

email: king@physics.unlv.edu

Anita Krishnamurthi

JILA, University of Colorado and National Institute of Standards and Technology, Campus Box

440, Boulder, CO 80309-0440

email: anitak@casa.colorado.edu

Mark H. Pinsonneault

Department of Astronomy, The Ohio State University, 140 W. 18th Ave., Columbus, OH 43210

email: pinson@astronomy.ohio-state.edu

ABSTRACT

The dispersion in lithium abundance at fixed effective temperature in young cool stars like the Pleiades has proved a difficult challenge for stellar evolution theory. We propose that Li abundances relative to a mean temperature trend, rather than the absolute abundances, should be used to analyze the spread in abundance. We present evidence that the dispersion in Li equivalent widths at fixed color in cool single Pleiades stars is at least partially caused by stellar atmosphere effects (most likely departures from ionization predictions of model photospheres) rather than being completely explained by genuine abundance differences. We find that effective temperature estimates from different colors yield systematically different values for active stars. There is also a strong correlation between stellar activity and Li excess, but not a one-to-one mapping between unprojected stellar rotation (from photometric periods) and Li excess. Thus, it is unlikely that rotation is the main cause for the dispersion in the Li abundances. Finally, there is a strong correlation between detrended Li excess and potassium excess but not calcium (perhaps supporting incomplete radiative transfer calculations (and overionization effects in particular) as an important source of the Li scatter. Other mechanisms, such as very small metallicity variations and

¹Current address

magnetic fields, which influence PM S Liburning may also play a role. Finally, we find no statistical evidence for a decrease in dispersion in the coolest Pleiades stars, contrary to some previous work.

Subject headings: open clusters and associations: individual (Pleiades) | stars: abundances, activity, atmospheres, interiors, late-type, rotation

1. Introduction

Predictions are made by standard stellar models (e.g., Bahcall & Ulrich 1988) about the surface abundances of elements in stars. However, there are indications that such models are incomplete. A case in point is the surface abundance of the element lithium (Li) in low mass stars, which is observed to decrease with time.

The solar meteoritic value for the Li abundance is 3.31 -0.04 (Anders & Grvesse 1989). A study of Li abundances in young, pre-main-sequence (PM S) T Tauri Stars (TTS) suggests a value of $\log N(Li) = 3.2 - 0.3$ (Magazzù, Rebolo, & Pavlenko 1992), consistent with the meteoritic value. While this is one indicator of the initial Li abundance, TTS abundance determinations are beset by complications due to their youth, such as uncertain T_e estimates and the presence of a circumstellar accretion disk. The study of stars in open clusters of different ages, like Persei (50 M yr) and the Pleiades (70-100 M yr), shows that there is nearly a uniform Li abundance of 3.2 for high mass stars (~7000 K).

It is known that surface Li depletion takes place during the PM S evolution of low mass stars due to Liburning via (p, γ) reactions at low temperatures of $T > 2.6 \times 10^6$ K. Surface depletion can occur in standard models through convective mixing if the base of the convection zone is hot enough to burn Li (Bodenheimer 1965, Pinsonneault 1997). Because PM S stars have deep convection zones, they burn Li during the PM S. As the depth of the convection zone is a function of mass (increasing with lower mass) Li is depleted on the main sequence only in lower mass stars (~0.9 M $_\odot$). However, the Pleiades evinces a large dispersion in surface Li abundance at a given color for $T_e < 5500$ K (e.g., Soderblom et al. 1993b). Standard stellar models are unable to reproduce this dispersion. Furthermore, open cluster observations indicate some depletion is observed on the main sequence as well, which is in conflict with standard models.

Because these models cannot fully explain the observed depletion patterns, additional mixing mechanisms seem necessary. Rotation provides one driving mechanism for such non-convective mixing, through meridional circulation (Tassoul 1978, Zahn 1992) and instabilities caused by differential rotation (Zahn 1983). Hence, rotation in stars has received much scrutiny as a possible agent of Li depletion and of the observed scatter in open cluster Li abundances at a given mass. Models which include rotational mixing (Pinsonneault, Kawaler, & Demarque 1990) are able to predict the dispersion seen in older systems, but not at young ages like that of the Pleiades

(Chaboyer, Demarque, & Pinsonneault 1995). The study of Li abundances is a rich and vast field, and there have been several efforts to study the correlation of surface Li abundances with rotation using stars in open clusters. Here, we concentrate on the connection between surface Li abundance and rotation using data in the young Pleiades cluster.

Because the Pleiades Li scatter is such a difficult obstacle in our understanding of early stellar evolution, a historical summary seems in order. Butler et al. (1987) studied a sample of 11 K-type stars in the Pleiades and determined that four rapid rotators had higher Li abundances than four slow rotators. They believed this consistent with the evolutionary picture that on arrival on the main sequence, stars had high rotation rates and high Li abundances (i.e., they arrived on the main sequence before there was time for rotational braking or Li depletion). As the star spun down, the Li abundance decreased as well. Hence, they concluded that the faster rotators were younger than the slower, hence less depleted.

A study of the distribution of rotational velocities of low-mass stars in the Pleiades by Staufer & Hartmann (1987) revealed that there was a wide range of rotation velocities in the Pleiades K and M dwarfs. They showed that the distribution of rotation velocities in the Pleiades could be reproduced quite well invoking angular momentum loss, without having to resort to a large age spread which is also in contrast with the narrow main-sequence seen among the low-mass Pleiades stars.

Soderblom et al. (1993b) carried out an extensive study of Li abundances in the Pleiades. They considered several possible explanations for the dispersion in the observed abundances, including observational errors and the effect of starspots. They concluded that the spread in Li abundances seen was real and not an artifact of other physical conditions. They found that the Li abundance was correlated well with both rotation and chromospheric activity, and speculated that rapid rotation was somehow able to preserve Li in stars. While they found some low $v \sin i$ systems with high Li abundances, it was possible that these stars are faster rotators simply seen at low inclination.

Balachandran et al. (1988) studied a sample of stars in the younger Persei cluster (50 Myr) and concurred with the picture of Li-poor stars as slow rotators. However, a comparison of the Pleiades to Per by Soderblom et al. (1993b) showed that while most stars had similar abundances, a significant number of stars in Per had abundances that were less than that in the Pleiades by 1 dex or more. This was difficult to understand until Balachandran et al. (1996) published a corrected list of Li abundances that culled all non-members from the sample, bringing consistency to the Pleiades and Per abundances.

Garcia Lopez et al. (1991a,b) added seven stars to the Butler et al. sample in the range $4500 > T_e > 5500$ K and asserted a clear connection between Li abundance and $v \sin i$. They also found that the correlation breaks down for temperatures cooler than 4500 K. In a subsequent paper in 1994, they enlarged their sample and further studied the correlation, concluding that their earlier assertion was correct (there were no rapid rotators with low Li abundances and there

was a clear relationship between $\log N(Li)$ and $v \sin i$. They did note three stars (H II 320, 380 and 1124) having low $v \sin i$ values and Li abundances comparable to those of the rapid rotators as counterexamples, but speculated these objects were rapid rotators seen at low inclination angles. It is to be noted that, when determining mean abundances for their rapid and slow rotator populations, they included the 3 stars with low $v \sin i$ and high Li abundances in their rapid rotator sample. While this does not change the qualitative result they obtained, it does affect the magnitude of the difference in abundance between the two populations. It also demonstrates that there is a range of abundances for slow rotators.

Jones et al. (1996a) derived Li abundances and rotation velocities for 15 late-K Pleiades dwarfs, and also found that the correlation between Li abundance and rapid rotation breaks down for cooler stars ($T_e < 4400$ K). Jones et al. (1997) determined rotational velocities and Li abundances in the 250 M yr old cluster M 34, intermediate in age between the young Pleiades (70{100 M yr) and the Hyades (500 M yr). They concluded that the Li depletion and rotation velocities were in between the Pleiades and Hyades values, and that the pattern seen in these clusters suggested an evolutionary sequence for angular momentum loss and Li depletion.

One could speculate that some of the Li dispersion in the Pleiades and Per may be due to NLTE effects and unknown effects of stellar activity on the Li I line formation (Houdebine & Doyle 1995; Russell 1996; but see Soderblom et al. 1993b). The structural effects of rotation might also be responsible for the Li depletion pattern. Martin & Claret (1996) included this ingredient in their models for masses of 0.7 and 0.8 M and were able to produce enhanced Li abundances for stars with high initial angular momentum as a result of less effective PMS Li destruction in rapid rotators (i.e., their models imply initially rapid rotators will have high Li abundances relative to the other stars at the same T_e at young ages). Angular momentum loss as well as rotationally-induced mixing could affect these models.

The questions we consider here are if there truly is a correlation between Li abundance and rotation rate in the Pleiades, what the nature of the correlation is, and if not, what might explain the abundance scatter. We start with a careful sample selection for our analysis, and examine various possible causes that might contribute to the dispersion (including errors in abundance determination). We then proceed to an analysis of the Li-rotation correlation and explore other possible correlations that might be masquerading as a Li-rotation correlation.

2. Pleiades Lithium Abundances

2.1. Sample Selection and Definition

Lithium abundances were derived from the datasets in the studies of Soderblom et al. (1993a; S93a) and Jones et al. (1996). The two studies were merged to form our starting sample with the latter data preferred in cases of overlap. Secondary stellar companions can affect photometric

colors from which T_e values are derived, activity levels, measured line strengths, and activity levels deduced spectroscopically. Thus, in order to look at the intrinsic Pleiades Li abundance dispersion unrelated (directly or indirectly) to the presence of a stellar companion, binary systems were excised from our sample. Cluster and interloping field binaries identified by Mamajek et al. (1992) and Bouvier et al. (1997) were removed from the starting sample. Two spectroscopic binaries not in these lists, but identified as such by S93a, were also removed.

The color-magnitude diagram of this refined sample was then inspected photometrically to identify binaries using the dereddened $B-V$ photometry described by Pinsonneault et al. (1998). We found H II 739 to be an obviously overluminous (or overly red) outlier in the V vs. $B-V$, V vs. $V-I$, and I vs. $V-I$ diagrams, and eliminated it from the refined sample. Finally, all stars with upper limits on the 6707 Li I line's equivalent width were eliminated. These upper limits, as censored data, complicate the ensuing statistical analysis. These stars are also the very hottest and very coolest in the sample. Their photometrically-inferred T_e values and model atmospheres may be slightly more uncertain than the other objects in the sample. Their elimination simplifies the analysis and reduces possible additional sources of uncertainty.

This final sample of 76 Pleiades stars is listed in the first column of Table 1. The extinction-corrected V magnitude and reddening-corrected ($B-V$) and ($V-I$) colors are given in the second, third, and fourth columns. The color-magnitude diagram of these stars evinces a tight main sequence, and is shown in Figure 1 (open circles) with a 100 Myr isochrone described in Pinsonneault et al. (1998) and assuming a distance modulus of 5.63 (Pinsonneault et al. 1998). The only possibly discrepant outliers remaining are: a) H II 686, which appears overluminous in the V vs. $B-V$ plane, but not the $V-I$ plane b) H II 676, which appears underluminous (or too blue) in the $V-I$ plane and perhaps $B-V$ also, and c) H II 2034, which appears underluminous (or too blue) in the $B-V$ plane, but not in $V-I$. There is no convincing evidence that these slight discrepancies are related to binarity. Rather, they may be due to relatively large photometric errors in one passband or to physical effects (e.g., increased red flux from spots) unrelated to binarity. Stars rejected as binaries are plotted as filled triangles; their general propensity to reside above the main sequence is evident.

Tab. 1
Fig. 1

2.2. Stellar T_e and Activity Measures

S93a and Jones et al. (1996) provide photometric T_e estimates for all of the stars in Table 1. We re-examine these for comparison and because of concern that chromospheric activity or starspots might affect the colors of young stars. We calculated T_e using our $(B-V)_o$ values and the relation from Soderblom et al. (1993b, equation 3): $T_e = 1808(B-V)_o^2 - 6103(B-V)_o + 8899$. Temperatures were also derived from our $(V-I)_o$ colors using the relation from Randich et al. (1997): $T_e = 9900 - 8598(V-I)_o + 4246(V-I)_o^2 - 755(V-I)_o^3$. Both of these relations are based on the data from Bessell (1979), and should provide self-consistent temperatures given self-consistent photospheric colors. Columns 5, 6 and 9 give the T_e values of S93a, and those

derived here from $(B - V)$ and $(V - I)$.

We adopt the $H\alpha$ - and Ca II infrared triplet-based chromospheric emission measurements from S93a as stellar activity indicators. These are the ratio of the flux (relative to an inactive star of similar color) in the $H\alpha$ and Ca II lines relative to the total stellar bolometric flux. Given canonical views of a relation between stellar mass and chromospheric emission on the main sequence, it is also of interest to measure the residual $H\alpha$ and Ca II flux ratios. That is, we wish to detrend the general relation between stellar mass and activity such that activity differences unrelated to large-scale mass differences can be quantified. This was done by fitting the $H\alpha$ and Ca II flux ratios as a function of $(V - I)$ color temperature with a linear relation², and subtracting this fitted flux ratio (computed at a given $V - I$) from the measured flux ratio of each star. The relation for the fitted $H\alpha$ flux ratio (used below) was found to be $\log R_{H\alpha} ; t = (0.00044742 T_e (V - I)) - 2.12515$. The relation for the Ca II flux ratio was found to be $\log R_{\text{Ca II}} ; t = (0.00021017 T_e (V - I)) - 3.50280$.

We find strong evidence that our T_e values (hence, assuming self-consistency of the color- T_e relations, the photometric colors) are affected by activity level. Figure 2 shows the difference between the $(B - V)$ - and $(V - I)$ -based T_e values versus the $H\alpha$ flux ratios (top panel) and the mass-independent residual $H\alpha$ flux ratios (bottom panel). A relation is seen in both panels, such that the lowest T_e differences are seen predominantly for the lowest flux ratios while the largest T_e differences are seen predominantly for stars having the largest flux ratios. The ordinary linear correlation coefficients are significant above the 99.9% confidence levels for both panels.

The binary stars (filled triangles) behave similarly to the single stars in both panels; on average, though, the binaries exhibit larger T_e residuals than the single stars. This systematic effect likely reflects the additional influence of fainter (hence cooler and redder) companions on the photometric colors. If this interpretation is correct, it could suggest that the handful of inactive single stars with significant T_e residuals in the upper left portion of both panels are unrecognized binaries.

Significant differences between the $(B - V)$ - and $(V - I)$ -based T_e estimates, the slight propensity for $(B - V)$ to yield larger temperatures, and the association of these properties with stellar activity seems to be a common property of young stars noted and discussed by others (e.g., Garcia Lopez et al. 1994; Randich et al. 1997; King 1998; Soderblom et al. 1999). Explanations for these observed properties in young stars are at least twofold: a) increased B-band flux due to boundary layer emission associated with a circumstellar disk (presumably not applicable for our near-ZAMS Pleiads), and b) increased I-band flux due to the presence of cool spots. It is straightforward to associate increased prevalence and surface coverage of spots with increasing activity, and $H\alpha$ emission (used here to quantify activity) has been associated with accretion of

² Quantitative comparison of the resulting R^2 values indicated that fits with higher order functions did not yield statistically improved descriptions of the flux ratio-color relations.

circum stellar material in young stars. Given that the Pleiades age (100 M yr) is an order of magnitude larger than inferred disk lifetimes for solar-type stars (Skrutskie et al. 1990), spots are the more likely cause of the temperature difference-activity relation in our Pleiades sample.

2.3. Lithium Abundance Determinations and Trending

Li abundances for all our Pleiads were determined from the measured 6707 line strengths and our preferred T_e value. A blending complex lies some 0.4 Å blueward of the Li doublet. In our stars, the typical contribution of these blending features is 10 mA, which is significantly smaller than typical Li line strength of 100 mA. The blending contribution was subtracted³ following the approach of S93a, who parameterized the contaminating line strength as a function of $(B - V)$ color. Here, we recast this parameterization as a function of T_e so that differences in our $(B - V)$ - and $(V - I)$ -based temperatures were consistently accounted for in the analysis.

Given the T_e values and the corrected Li line strengths, abundances were calculated using Table 2 from S93a. This was done by fitting a surface map of the equivalent width-temperature-abundance grid of S93a using high order polynomials. The internal interpolation accuracy is generally a few thousandths of a dex⁴. Columns 8 and 11 of Table 1 give the derived Li abundances⁵ for our $(B - V)$ -based T_e , and for our $(V - I)$ -based T_e .

At the Pleiades age, PMS Libuming has significantly depleted the initial photospheric Li content of many of our stars. Moreover, this PMS depletion is a sensitive function of mass (or T_e) with less massive stars having depleted more Li due to deeper convection zones and longer PMS evolutionary timescales. In examining star-to-star Li abundance differences connected with parameters such as rotation or activity, we must remove this general large-scale trend in the abundance vs. T_e plane.

The procedure is illustrated in Figures 3 and 4, which shows the Pleiades Li abundances

³Deblending corrections were not applied to any stars taken from Jones et al. (1996) following their claim that instrumental resolution was sufficient to separate the Li line and blending complex. While it is not clear to us that this is true given that some of their objects have appreciable rotation (see their Figure 1), it does not affect the present results inasmuch as the Jones et al. rapid rotators have Li line strengths significantly larger than those expected of the blending complex.

⁴The two hottest single stars have T_e values significantly outside the curve of growth grids provided by S93a. Extrapolation to these temperatures with high order polynomials leads to errantly low abundances by a few tenths of a dex. To the extent that we are mainly interested in the cooler Pleiads and that we are only interested in the differential star-to-star Li abundances (i.e., large scale abundance morphology with T_e is removed later), these known errors are unimportant for the present analysis. In the case of these two stars (H II 133 and 470), we simply caution those who would use our absolute abundances, and also note that the few much smaller extrapolations to lower T_e outside the S93a grid are not believed to be affected by any substantial amount.

⁵by number, relative to hydrogen, on the usual scale with $\log N(H) = 12$:

versus our $(B - V)$ - and $(V - I)$ -based T_e . The familiar and large (3 orders of magnitude) abundance depletion over 2000 K of T_e is seen in Figure 3. The mean trend is shown by the dashed line, which is a fourth order Legendre polynomial fitted to the single star data after rejecting 3 outliers. Fourth order fits were also conducted for the data based on the S93a temperatures and our $(B - V)$ -based values. These fits provide a mean fiducial Li abundance at any given T_e to which observed abundances (calculated assuming the same source of T_e) can be compared to infer and measure a relative Li "enhancement" or "depletion" for each star as shown in Figure 4. For $(V - I)$ -based temperatures, the approximation to the fit shown in Figure 3 is given by: $\log N(Li) = 10.8602 + (2.9785 \cdot 10^{-3} T) + (1.1736 \cdot 10^{-7} T^2) - (3.8181 \cdot 10^{-11} T^3)$. For $(B - V)$ -based temperatures, the approximation to the fit shown in Figure 3 is given by: $\log N(Li) = 10.9959 + (2.8360 \cdot 10^{-3} T) + (1.7354 \cdot 10^{-7} T^2) - (4.2744 \cdot 10^{-11} T^3)$

2.4. Errors

Uncertainties in the Li abundances were estimated from those in T_e and equivalent width. Here, we are only interested in the internal errors which affect the star-to-star Li abundances. A measure of the internal uncertainties in the T_e estimates is provided by the estimates from the $(B - V)$ and $(V - I)$ colors. For the single stars, the difference in the two color-temperatures exhibits a per star standard deviation of 108 K. Assuming equal contributions from both $(B - V)$ and $(V - I)$, this suggests an internal error of 76 K in the T_e of any one Pleiad derived from any one color. This uncertainty was translated to a Li abundance error by re-deriving abundances with T_e departures of this size. The adoption of identical errors in $(B - V)$ and $(V - I)$ -based T_e values is a simplifying assumption (though one likely true within a few tens of K). Inasmuch as our conclusions are the same using either the $(B - V)$ or $(V - I)$ colors, it is not a critical one for this work.

The other significant source of uncertainty is in the Li line measurements. For S93a line strengths (the majority of our sample), uncertainties come from their own quality measures: a (12 mA), b (18 mA), c (25 mA), and d (40 mA). Jones et al. (1996) state that their uncertainties range from 5-20 mA and depend largely on projected rotational velocity. Assuming this range and the stars' $vsini$ values, we have adopted the reasonable values shown in column 12 of Table 1. Given S93a's note that the equivalent widths of Butler et al. (1987) may have to be regarded with caution, and the typical expected uncertainties from Poisson noise expected from their S/N and resolution, we have assigned an uncertainty of 30 mA in these line strengths. Based on the S/N, resolution, and $vsini$ values of the observations from Boesgaard et al. (1988), we have adopted a conservative uncertainty of 5 mA for their data. In a similar fashion, we assigned uncertainties of 25 mA to the equivalent widths from Pilachowski et al. (1987). The line strength uncertainties were translated to Li uncertainties by re-deriving abundances with the adopted equivalent width departures.

Final Li abundance uncertainties, shown in Figures 3 and 4, are calculated by summing the

two errors in quadrature, and listed in columns 13 and 14 of Table 1. We emphasize that for the purpose of looking at the star-to-star Li abundance differences in cool Pleiades, the effects of T_e errors are minimized. This is because the movement of a star in the T_e -Li plane due to T_e errors is very nearly along the cool star depletion trend for $T_e < 5800$ K. To take into account this correlation in looking at the differential Li abundances (i.e., the actual values versus an expected value from a fitted trend to the data), the abundance errors due to departures in T_e were combined with the slope of the fitted Li versus T_e trend at the T_e of each star. The total uncertainties in the differential Li abundances are given in the final two columns of Table 1.

2.4.1. Li Abundance Scatter

Large scatter in the star-to-star Li abundances is apparent in Figures 3 and 4. Comparison of the observed scatter with that expected from the estimated uncertainties indicates that the spread is statistically significant. The presence of real global scatter was considered by comparing the variance of the differential Li abundances with that based on the uncertainties given in Table 1. The sizable reduced chi-squared statistic ($\chi^2 = 12.78$, $N = 72$) indicates probabilities of the observed variance ($s(\text{Li})^2 = 0.13 \text{ dex}^2$) occurring by chance are in nitesimal.

Additional analysis was carried out by binning in T_e . For both the (B-V) and (V-I) based results, we broke the data up into 5 T_e ranges following natural breaks in the estimated T_e values which yielded comparable sample sizes (10-15 stars) in each bin. The results for both the (B-V) and (V-I) data are similar.

We find that stars in the hottest bin (bin E': 6172-6984 K and 6107-6928 K for B-V and V-I) exhibit a variance that is larger than the expected value at only the 94% confidence level. The stars in the adjacent cooler bin (bin D': 5567-6048 K and 5521-6021 K for B-V and V-I) exhibit a variance in the Li abundances significantly larger than expected from the uncertainties at the > 99.93% confidence level. The differential Li abundances in the remaining three cooler bins (bin C': 4899-5477 K and 4996-5452 K; bin B': 4507-4815 K and 4542-4746 K; bin A': 3955-4332 K and 3867-4343 K) all show observed variances significant at considerably higher confidence levels.

An important claim by Jones et al. (1996) in their study of Pleiades Li abundances is a progressive decline in the dispersion of the Li abundances as one proceeds from the late G dwarfs, to the early-to-mid K dwarfs, and finally to the later K dwarfs. We find, however, that quantitative analysis fails to provide much support for such a conclusion. F-tests of the observed variances indicate that differences of the differential Li abundance dispersions in our cooler three bins are statistically indistinguishable. The differences between the bin B and bin A stars' variances are significant at only the 71.5% and 78.0% confidence levels for the B-V and V-I datasets. Differences between the bin C and bin B stars' variances are different at only the 72.7% and 75.0% confidence levels. It should be noted that these comparisons ignore the observed Li upper

lim its prevalent for the coolest (bin A) Pleiads. The stars with upper lim its lie at the lower edge of the observed Li abundances (figure 4 of Jones et al.). Ignoring this censored data may lead to an underestimate of the true dispersion for the coolest Pleiads, making our conclusion of no significant difference in the magnitude of star-to-star abundance scatter for the late G to late K Pleiads a conservative one. Larger samples and improved upper lim its (or detections) would clarify this important issue.

3. Nature of the Li-rotation correlation

3.1. Projected rotational velocity

Extant studies of Li-rotation correlations have employed $v \sin i$ measurements, which yield only a lower limit to the rotational velocity due to the unknown angle of inclination, i . In Figure 5, our $V - I$ -based absolute and differential Li abundances are plotted against the projected velocity measurement $v \sin i$. The top two panels (a and b) show the data for all T_e . The bottom two panels (c and d) show data with $4500 \leq T_e \leq 5500$ K, which is the temperature range in which a clear connection between Li abundance and $v \sin i$ was asserted by Garcia Lopez et al. (1994). It is seen that while there is a range of abundances at the lower values of the rotation velocity, the rapid rotators ($v \sin i > 30 \text{ km s}^{-1}$) do show a tendency to have higher Li abundances in the intermediate T_e range (panel d).

3.2. Rotational Period

The Pleiades now has many members with photometrically-determined rotation periods (Kishnamurthi et al. 1998), which are free of the ambiguity associated with inclination angle. Hence, it is now possible to consider the true nature of the correlation between rotation and Li abundance. For example, we find a slowly rotating star (H II 263, $P = 4.8$ d) that has a high Li abundance. Furthermore, two of the three stars (H II 320 and 1124) in the Garcia Lopez et al. (1994) study with low $v \sin i$ and high Li abundances also have measured rotation periods of 4.58d and 6.05d respectively. Thus, there are several cases where high Li abundance in stars with low $v \sin i$ is not due to inclination angle effects; Li overabundances are not solely restricted to rapid rotators. This is apparent in Figure 6, where the surface Li abundance is plotted against rotation period, P_{rot} , instead of $v \sin i$. In particular, we draw attention to the large range in abundances seen at longer rotation periods (> 4.0 days; panels b and d). Thus there exist at least a few Pleiads which are true slow rotators, but have high Li abundances.

We next examined the proposal by Garcia Lopez et al. (1994) that there is a very clear relationship between rotation and $\log N(\text{Li})$ for stars with $M = 0.7-0.9 M_{\odot}$. Figure 7 shows the $V - I$ -based Li abundances versus mass for Pleiads with photometrically-measured rotation rates.

The symbol size is proportional to the rotation period. When rotational periods are considered rather than $v \sin i$ measurements, a true range of Li abundances with rotation is seen in the mass range 0.7-0.9 M \odot (there are genuine slow rotators with abundances similar to the fast rotators. Thus, there appears to be a range of rotation at all abundances. Hence, P_{rot} is essential to study the true correlation.

Fig. 7

3.3. Structural effects of rotation

Rapid rotation affects the structure of a star and hence the derived mass at a given T_e (Endal & So 1979). The structural effects of rotation would alter a star's color such that rapidly rotating objects would be redder, hence perceived as cooler, and thus be assigned a lower mass. We therefore examined the abundances as a function of mass rather than effective temperature.

To investigate this issue, it was necessary to construct stellar models for different disk lifetimes (Krishnamurthi et al. 1997). We ran models for $\tau_{\text{crit}} = 5$ and 10 to represent fast rotators and the slow rotators. The rotation-corrected masses were derived by interpolation in the models across effective temperature and rotation velocity for different disk lifetimes. We found that the percent change in mass is small (5%) even for the most rapidly rotating star in the Pleiades (H II 1883, $v \sin i = 140 \text{ km s}^{-1}$). The change is between 1% and 2% for stars with $v \sin i$ in the 50-100 km s^{-1} , and < 1% for $v \sin i = 50 \text{ km s}^{-1}$. These small alterations fail to eliminate the Li dispersion, which sets in at $M < 0.9 M_\odot$ in the Li-mass plane. Thus, the structural effects of rotation on the derived mass-temperature relation are not large enough to account for the Pleiades Li abundance dispersion.

These results differ with those of Martin & Claret (1996), who also explored the structural effects of rotation and found enhanced Li abundances for stars with high initial angular momentum. This is not seen in our models, which predict small rotational structure effects on the Pleiades Li abundances, similar to the models of Pinsonneault et al. (1990). Mendes et al. (1999) have noted the conflict between the results of Martin & Claret (1996) and Pinsonneault et al. (1990), and considered the hydrostatic effects of rotation on stellar structure and Li depletion using their own stellar models. Their results are in agreement with Pinsonneault et al. (1990), and they too find that hydrostatic effects are too small to explain the observed Li abundance spread in the Pleiades.

4. Li and Stellar Activity

4.1. Li and chromospheric emission

Since the large Pleiades Li spread is in such a young cluster, one may wonder if its long-sought explanation is related to stellar activity. Additionally, since rotation and activity are well-correlated, a Li-activity relation may be masquerading as a Li-rotation relation instead. Here,

we discuss if magnetic activity indicators such as chromospheric emission (CE) are correlated with the Li abundance. Several studies have pointed out that activity is correlated with the Li abundance (e.g., Soderblom et al. 1993b, Jones, Fischer & Stau er 1996b). There have also been some studies speculating that CE affects the apparent abundance of Li (e.g., Houdébaine & Doyle 1995) and hence may be at least partly responsible for the dispersion.

Figure 8 contains our results, and shows the V - I-based differential Li abundances versus the Ca II infrared triplet fluxes (top panel) and residual fluxes (bottom panel). A relation is seen in both panels, such that the lowest $\log N(Li)$ differences are seen predominantly for the lowest flux ratios while the largest $\log N(Li)$ differences are seen predominantly for stars having the largest flux ratios. The ordinary correlation coefficients are significant at the 99.7% and 99.9% confidence levels for the chromospheric Ca fluxes and residual fluxes, suggesting a significant relation between chromospheric activity differences and Li abundance differences (though not necessarily causal).

4.2. Spreads in Other Elements

Important clues to the cause of the Pleiades Li abundance scatter can be found from examination of other elements not destroyed in stellar interiors like 7Li . Variations in such abundances may signal effects other than differential Li processing, and perhaps point to an illusory difference caused by inadequate treatment of line formation.

4.2.1. Potassium

One of the most useful features for this purpose is the 7699 K I line. The usefulness of this feature is two-fold. First, there is the similarity in electronic configuration with the Li I atom and the fact that this particular K transition and the 6707 Li I are both neutral resonance features. Second, the interplay of abundance and ionization effects leads to the happy circumstance that the line strengths of these two features are comparable in Pleiades dwarfs. Thus, line formation for both features should be similar in many respects.

The K I line strengths were taken from S93a and Jones et al. (1996). These were then plotted versus T_e as derived from both B - V and V - I. The relation was well fit by a 4th order Legendre polynomial approximated by the relation: $EW(K) = 9098.151 (4.126458 T) + (6.381173 \cdot 10^{-4} T^2) (3.308942 \cdot 10^{-8} T^3)$ for the B - V colors and by the relation: $EW(K) = 8926.171 (4.170605 T) + (6.702972 \cdot 10^{-4} T^2) (3.642286 \cdot 10^{-8} T^3)$ for the V - I colors. These fits showed considerable scatter (the line strength dispersion was 55 mA, which is considerably larger (and statistically significant) than even the maximum equivalent width errors estimated by S93a. So scatter is present in the potassium data as well.

Differential K I equivalent widths ([observed / tted] / tted) are plotted against the differential Li abundances in Figure 9. A correlation between the values is present, though with considerable scatter. The one-sided correlation coefficients are significant at the 99.0 and 98.3% confidence levels for the (B V) and (V I)-based results. Such a correlation (of whatever magnitude), however, may arise not from some physical mechanism; instead, it may simply reflect correlated measurement errors.

Fig. 9

Like the differential Li abundances, the differential K I line strengths are correlated with activity measure. Figure 10 shows the differential K I equivalent width versus the Ca II fluxes (top panel) and residual fluxes (bottom panel). The correlations are analogous to those seen for the differential Li abundances in Figure 8, and are significant at the 98.5% (top panel) and 99.9% (bottom panel) confidence levels.

Fig. 10

4.2.2. Calcium

To examine the possibility of correlated measurement errors, we considered the line strengths of the 6717 Ca I feature taken from S93a. These were tted against T_e in the same manner as the K I equivalent widths. The relations are given by: $EW(Ca) = 4203.706 (1.859218 T) + (2.888087 \cdot 10^{-4} T^2) - (1.538325 \cdot 10^{-8} T^3)$ for the B V colors and by $EW(Ca) = 2978.740 (1.249348 T) + (1.887209 \cdot 10^{-4} T^2) - (9.973237 \cdot 10^{-9} T^3)$ for the V I colors. The scatter associated with these ts is 20 m A, which is consistent with the S93a uncertainties. Interestingly, unlike Li and K, there is no evidence for scatter in the calcium data above the measurement uncertainties. Differential Ca I equivalent widths are plotted against the differential Li abundances in Figure 11. The relation is at. Unlike K, there is no significant correlation (the ordinary correlation coefficients are significant at only the 80% confidence level).

Fig. 11

This indicates to us that the correlated scatter in Li and K line strengths is not due to measurement errors. Rather, we suggest that some physical mechanism affecting the details of line formation not included in standard LTE model photosphere analyses is the cause. Such a mechanism, if having star-to-star differences, may be the dominant source of the Li abundance scatter in Pleiades dwarfs. Since activity evinces such differences, it may naturally provide such a mechanism. Houdebine & Doyle (1995; HD 95) demonstrate that formation of the 6707 Li I line is sensitive to activity in M dwarfs. The extent of these effects depends on the relative coverage of plages and spots. HD 95 note the particular importance of the role of ionization in reducing the resonance line's optical depth. In late G and K dwarfs like those showing scatter in the Pleiades, star-to-star variations in departures of both photoionisation and collisional ionization from that predicted by model photospheres might introduce significant star-to-star variations in the derived Li abundance⁶. Interestingly, King et al. (1999) find element-to-element abundance differences in

⁶Overionization from photospheric convective inhomogeneities has been discussed in the context of Population II

two cool ($T_e = 4500$ K) Pleiades dwarfs and a similarly cool NGC 2264 PM S member which are ionization potential dependent. We suggest that current evidence implicates non-photospheric ionization differences as a likely source of star-to-star Li variations in the Pleiades.

5. Other Mechanisms and Concerns

5.1. Metal abundance variations

Variations in abundances of other elements can affect stellar Li depletion via the effects of stellar structure on PM S Libuming. For example, Figure 3 of Chaboyer, Demarque, & Pinsonneault (1995), indicates that very small metal abundance differences of, say, 0.03 dex lead to substantial ($> 0.3 - 0.4$ dex) differences in PM S Libuming for $T_e < 4500$ K.

Extant studies (Boesgaard & Friel 1990; Cayrel, Cayrel, & Cambpell 1988) of Pleiades F- and G-star iron abundances (which cannot simply be equated with "metallicity" when it comes to PM S Libumption; Swenson et al. 1994) suggest no intrinsic scatter larger than 0.06-0.10 dex. The photometric scatter of the single stars in the color-magnitude diagram might allow a metallicity (or, perhaps more properly, those elements which are dominant electron donors in the stellar photospheres) spread of 0.05 dex. While small, these constraints would still permit substantial Li abundance spreads for cool Pleiads. Additionally, abundances of elements which may have a large impact on PM S Libumption but little effect on atmospheric opacity (e.g., oxygen) have yet to be determined in cool Pleiades dwarfs.

However, the Li spread in the Pleiades extends to T_e values substantially hotter than 4500 K. At hotter T_e values, model PM S Libuming is less sensitive to metallicity. For example, in the range 5000-5200 K, the observed Li abundance spread would require "metallicity" differences approaching a factor of two. Such spreads would be surprising indeed, and not expected based on the limited results of extant Fe analyses of hotter cluster dwarfs. Abundance differences (of a large number of elements) of this size would not be difficult to exclude with good quality spectra as part of future studies.

5.2. Magnetic Fields

Ventura et al. (1998) have recently investigated the effects of magnetic fields in stellar models and PM S Libumption. They find that even small fields are able to inhibit convection, and thus PM S Libumption. They suggest that a dynamo generated magnetic field linked to rotational velocity (thus, presumably yielding an association between activity and rotation given conventional wisdom) would result in ZAMS star-to-star Li variations that mirror differences in star-to-star

rotational (and presumably activity) differences. As these authors admit, the fits of their magnetic models to the Li-T_e morphology and significant scatter of the Pleiades observations are not "perfect" or "definitive"; however, the qualitative agreement and ability to produce star-to-star scatter and general relations between Li abundance and rotation and activity are encouraging. Continued observations (especially detailed spectroscopic abundance determinations of various elements in numerous Pleiads) and theoretical work will be needed to establish the degree to which the Pleiades Li spread is illusory or real and, if the latter, its cause(s).

6. Summary and Conclusions

The very large dispersion in Li abundances at fixed T_e in cool (T < 5400 K) Pleiads is a fundamental challenge for stellar evolution because standard stellar models of uniform age and abundance are unable to reproduce it. A variety of mechanisms (rotation, activity, magnetic fields, and incomplete knowledge of line formation) have been proposed to account for this scatter. Here, we construct a sample of likely single Pleiads and consider this problem with: a) differential Li abundances relative to a mean T_e trend b) rotational periods instead of projected rotational velocities c) chromospheric emission indicators, and d) line strengths of other elements.

We calculated T_e values from both (B - V) and (V - I) on a self-consistent scale based on the calibrations of Bessell (1979). We find differences in the two T_e values and these are significantly correlated with both general activity level and with differences in activity, suggesting that surface inhomogeneities may noticeably affect stellar colors. Our results are consistent with a growing body of evidence of significant differences between (B - V)- and (V - I)-based T_e values, a propensity for (B - V) to yield larger T_e values, and a relation of these characteristics with activity in young stars from 5 M yr old PM S stars in NGC 2264 (Soderblom et al. 1999) to PM S stars in the 30 M yr old IC 2602 (Randich et al. 1997) to ZAMS stars in the 100 M yr old Pleiades.

However, the similarity between the sensitivity of the derived Li abundance to T_e and the clusters' physical Li-T_e morphology means that even substantial T_e errors are not a significant source of star-to-star Li scatter. Nor are observational errors. Comparison of the scatter in the differential Li abundances with errors from T_e and line strength uncertainties indicates an infinitesimal probability that the observed scatter occurs by chance. We find significant scatter in the Li abundances below 6000 K; it is significantly larger, though, below 5500 K. Statistical analysis fails to support previous claims of smaller scatter in the late K dwarfs relative to the late G and early-mid K dwarfs.

There is a spread of Li abundance at low v sin i, whereas the rapid projected rotators tend to have larger differential Li abundances in the range 4500 < T_e < 5500. However, use of photometric rotation periods (free from uncertainties in the inclination angle i) indicates there is not a one-to-one mapping between differential Li abundance and rotation. The stars H II 263, 320, and

1124 are examples of stars with Li excesses but slow rotation ($P = 4.6 - 6.1$ d). In contrast to previous claims based on $v \sin i$, the rotation periods indicate a true range of Li abundance with rotation in the mass bin $0.7-0.9 M_{\odot}$.

Using the theoretical framework of Krishnamurthi et al. (1997), we constructed stellar models to investigate the hydrostatic effects of rotation on stellar structure and PM S Libum. As shown in Figure 8, these models fail to account for the Pleiades Li dispersion, which is in agreement with the independent conclusions of Mendes et al. (1999).

We find that the star-to-star differences in Pleiades Li abundances are correlated with activity differences, as measured from Ca II infrared triplet flux ratios, at a statistically significant level. Moreover, the Li differences are significantly correlated with differences in the strengths of the 7699 K I resonance feature. This seems to not be due to correlated measurement errors since the Li differences show no correlation with the 6717 Ca I line strength residuals. This is a significant result given similarities in the Li and K feature's atomic properties and line strengths. We suggest that incomplete treatment of line formation, related to activity differences, plays a significant role in the Li dispersion (i.e., that part of the dispersion is illusory. As emphasized by Houdebine & Doyle (1995), the formation of the Li I feature is sensitive to ionization conditions. If chromospheric activity variations can produce significant variations in photo- and collisional-ionization in the Li I line formation region not accounted for by LTE analyses using model photospheres, this may lead to errors in the inferred abundance. Relatedly, we note the results of King et al. (1999) who found ionization potential-dependent effects in the elemental abundances of two cool (T_e) Pleiads and a similarly cool NGC 2264 PM S star.

If such conjecture is correct, we expect that somewhat older (less active) cluster stars will exhibit less Li dispersion. This seems to be the case for the 800 M yr old Hyades cluster (Thorburn et al. 1993) and perhaps also for the mid-G to mid-K stars in M 34 (Jones et al. 1997). These clusters still exhibit scatter, and this may be real and due to differences in depletion from structural effects of rotation (Mendes et al. 1999), magnetic fields (Ventura et al. 1998), small metallicity variations (± 5.1), main sequence depletion due to angular momentum transport from spin-down (Pinsonneault et al. 1990; Charbonneau et al. 1992) or a planetary companion (Cochran et al. 1997), and photospheric accretion of circumstellar/planetary material (Alexander 1967; Gonzalez 1998). The amount of scatter expected in even older clusters is less clear. If, e.g., rotationally-induced mixing acts over longer timescales than the scatter may well increase again; indeed, the substantial Li scatter in M 67 solar-type stars observed by Jones et al. (1999) could indicate that this is the case.

These authors called attention to the possible pattern of very large Li scatter in young clusters, considerably reduced scatter in intermediate-age clusters, and increased scatter in older clusters. In the scenario we envision, variations in activity-regulated ionization of the Li I atom may be responsible for the majority of (mostly illusory) star-to-star Li differences in near-ZAMS and younger stars; of course, this does not exclude a (lesser) role from other variable mechanisms

in uencing PM S Libuming. If the decline in the activity level of intermediate-age stars reduces the importance of variable ionization, then the (smaller) Li scatter in these stars could arise from variations in PM S Libuming due to, e.g., the hydrostatic effects of rotation on stellar structure, inhibition of convection by magnetic fields, and small metallicity variations; additional contributions may come from processes just beginning to become effective for ZAMS stars such as rotationally-induced mixing and planetary/circumstellar accretion. In older stars such as M 67, the increase in scatter (and overall Li depletion) is then a product of processes efficiently acting on the main-sequence proper such as rotationally-induced mixing and/or photospheric accretion.

Distinguishing specific mechanisms and their relative importance for Li depletion and scatter at a given age will require continuing observational and theoretical efforts. Important advances on the theoretical front are at least three-fold: continued investigation of the role of magnetic fields in PM S Lib depletion, realistic models of atmospheres which include chromospheres, and detailed NLTE abundance calculations which employ these models. On the observational front, continued observations of Li in a variety of clusters spanning a range in age and metallicity are needed. We believe that particularly important observational work to be accomplished includes the determination of photometric periods in more cluster stars, detailed abundances of numerous elements (in particular, using both ionization sensitive and ionization insensitive features and elements) in cluster stars, quantification of even small "metal" (not just Fe) abundance spreads in cluster stars, and the association between planetary systems and parent star Li and light metal abundances.

R E F E R E N C E S

Anders, E., & Grøvæsse, N. 1989, in *Geochemical and Cosmochimical Acta* 53:197-214

Alexander, J.B. 1967, Observatory, 87, 238

Balachandran, S., Lambert, D.L., & Stauder, J.R. 1988, ApJ, 333, 267

Balachandran, S. 1995, ApJ, 446, 203

Bahcall, J.N., & Ulrich, R.K. 1988, RvMP, 60, 297

Bessell, M.S. 1979, PASP, 91, 589

Bodenheimer, P. 1965, ApJ, 142, 451

Boesgaard, A.M., Budde, K.G., & Ramsay, M.E. 1988, ApJ, 327, 389

Boesgaard, A.M., & Friel, E.D. 1990, ApJ, 351, 467

Bouvier, J., Rigaut, F., & Nadeau, D. 1997, A&A, 323, 139

Butler, R.P., Cohen, R.D., Duncan, D.K., & Marcy, G.W. 1987, ApJ, 319, L19

Cayrel, R., Cayrel de Strobel, G., & Campbell, B. 1988, in "The Impact of Very High S/N Spectroscopy on Stellar Physics", eds. G. Cayrel de Strobel and M. Spite, (Dordrecht: Kluwer), p. 449

Chaboyer, B., Demarque, P., & Pinsonneault, M. H. 1995, *ApJ*, 441, 876

Charbonnel, C., Vauclair, S., & Zahn, J.-P. 1992, *A & A*, 255, 191

Cochran, W. D., Hatzes, A. P., Butler, R. P., & Marcy, G. W. 1997, *ApJ*, 483, 457

Endal A. S., & So a, S. 1979, *ApJ*, 232, 531

Garcia Lopez, R. J., Rebolo, R., Magazzu, A., & Beckmann, J. E. 1991a, *Mem. Soc. Astr. Ital.*, 62, 187

Garcia Lopez, R. J., Rebolo, R., Beckmann, J. E., & Magazzu, A. 1991b in "The Sun and Cool Stars: activity, magnetism, dynamos", I. Tuominen, D. Moss, & G. R. Rüdiger (eds.), *Lecture Notes in Physics*, Vol. 380, (Berlin: Springer), p. 443

Garcia Lopez, R. J., Rebolo, R., & Martin, E. L. 1994, *A & A*, 282, 518

Gonzalez, G. 1998, *A & A*, 334, 221

Houdebine, E. R., & Doyle, J. G. 1995, *A & A*, 302, 861

Jones, B. F., Shetrone, M., Fischer, D., & Soderblom, D. R. 1996a, *AJ*, 112, 186 (JSFS)

Jones, B. F., Fischer, D., Shetrone, M., & Soderblom, D. R. 1996b, *AJ*, 114, 352

Jones, B. F., Fischer, D. A., & Stau er, J. R. 1996b, *AJ*, 112, 1562

Jones, B. F., Fischer, D., & Soderblom, D. R. 1999, *AJ*, 117, 330

King, J. R. 1998, *AJ*, 116, 254

King, J. R., Soderblom, D. R., Fischer, D., & Jones, B. F. 1999, in preparation

Krishnamurthi, A., Pinsonneault, M. H., Barnes, S., & So a, S. 1997, *ApJ*, 480, 303.

Krishnamurthi, A., Temdrup, D. M., Pinsonneault, M. H., Sellgren, K., Stau er, J. R., Schild, R., Backman, D. E., Beisser, K. B., et al. 1998, *ApJ*, 493, 914

Kurucz, R. L. 1995, *ApJ*, 452, 102

Magazzu, A., Rebolo, R., & Pavlenko IV 1992, *ApJ*, 392, 159

Mendes, L. T. S., D'Antona, F., & Mazzitelli, I. 1999, *A & A*, 341, 174

Mermilliod, J.-C., Rosvick, J. M., Duquennoy, A., & Mayor, M. 1992, *A & A*, 265, 513

Pilachowski, C. A., Booth, J., & Hobbs, L. M. 1987, *PA SP*, 99, 1288

Pinsonneault, M. H., Kawaler, S., & Demarque, P. 1990, *ApJS*, 74, 501

Pinsonneault, M. 1997, *ARA A*, 35, 557

Pinsonneault, M. H., Stau er, J., Soderblom, D. R., King, J. R., & Hanson, R. B. 1998, *ApJ*, 504, 170

Randich, S., Aharpour, N., Pallavicini, R., Prosser, C. F., & Stau er, J. R. 1997, *A & A*, 323, 86

Russell, S. C. 1996, *ApJ*, 463, 593

Skrutskie, M. F., Dutkevitch, D., Strom, S. E., Edwards, S., Strom, K. M., & Shure, M. A. 1990, *AJ*, 99, 1187

Soderblom, D. R., Jones, B. F., Balachandran, S., Stau er, J. R., Duncan, D. K., Fedele, S. B., & Hudon, J. D. 1993a, *AJ*, 106, 1059

Soderblom, D. R., Stau er, J. R., Hudon, J. D., & Jones, B. F. 1993b, *ApJS*, 85, 315

Soderblom, D. R., King, J. R., Siess, L., Jones, B. F., Fischer, D. 1999, *AJ*, in press

Stau er, J. R., & Hartmann, L. W. 1987, *ApJ*, 318, 337

Swenson, F. J., Faulkner, J., Iglesias, C. A., Rogers, F. J., & Alexander, D. R. 1994, *ApJ*, 422, L79

Tassoul, J.-L. 1978, in "Theory of Rotating Stars", Princeton: Princeton University Press.

Thorburn, J. A., Hobbs, L. M., Deliyannis, C. P., & Pinsonneault, M. H. 1993, *ApJ*, 415, 150

Ventura, P., Zeppieri, A., Mazzitelli, I., & D'Antona, F. 1998, *A & A*, 331, 1011

Zahn, J.-P. 1983, in "Astrophysical Processes in Upper Main Sequence Stars", eds. B. Hauck and A. Maeder, Geneva: Geneva Observatory, 253

Zahn, J.-P. 1992, *A & A*, 265, 115

TABLE 1
PLEIADES SINGLE STAR SAMPLE USED

Name (H II)	V	B-V	V-I	T_{eff} (S93a)	T_{eff} (B-V)	EW (B-V)	Li (B-V)	T_{eff} (V-I)	EW (V-I)	Li (V-I)	σ (EW)	σ (Li) (B-V)	σ (Li) (V-I)	σ (Δ Li) (B-V)	σ (Δ Li) (V-I)	Prot (d)
25	9.35	0.44	0.52	6560	6564	57	2.99	6471	57	2.92	5	0.07	0.07	0.09	0.09	...
34	11.84	0.88	0.92	4900	4928	134	1.94	4996	135	2.03	18	0.14	0.14	0.11	0.10	6.553: (1)
152	10.60	0.645	0.685	5700	5715	150	2.92	5760	150	2.97	12	0.10	0.10	0.08	0.08	4.12 (3)
164	9.40	0.46	0.54	6480	6474	59	2.95	6376	58	2.86	5	0.07	0.08	0.09	0.09	...
193	11.18	0.75	0.80	5320	5339	148	2.51	5352	148	2.52	12	0.11	0.11	0.07	0.07	...
250	10.59	0.645	0.68	5740	5715	141	2.87	5779	141	2.93	12	0.10	0.10	0.08	0.08	...
253	10.59	0.64	0.75	5700	5734	186	3.17	5521	185	2.93	18	0.14	0.14	0.12	0.11	...
263	11.51	0.84	0.90	5060	5048	290	3.10	5051	290	3.10	12	0.13	0.13	0.09	0.09	4.82 (7)
293	10.665	0.675	0.71	5640	5603	125	2.66	5666	125	2.72	12	0.11	0.11	0.08	0.08	4.2: (6)
296	11.33	0.80	0.86	5180	5174	278	3.17	5166	278	3.16	12	0.13	0.13	0.09	0.09	2.53 (3)
314	10.48	0.62	0.70	5840	5810	167	3.12	5703	166	3.01	18	0.13	0.13	0.12	0.11	1.48 (5,6)
324	12.87	1.01	1.23	4560	4579	210	1.90	4343	210	1.58	15	0.14	0.13	0.09	0.10	0.41 (2)
380	13.21	1.17	1.34	4240	4233	191	1.31	4186	190	1.26	18	0.14	0.13	0.12	0.12	...
405	9.72	0.50	0.58	6320	6300	81	2.99	6194	81	2.90	25	0.22	0.22	0.22	0.22	...
430	11.27	0.77	0.80	5240	5272	151	2.45	5352	151	2.54	18	0.14	0.14	0.10	0.11	...
489	10.295	0.585	0.67	5920	5947	127	3.00	5818	127	2.88	12	0.10	0.10	0.09	0.08	...
514	10.61	0.665	0.705	5660	5640	135	2.76	5684	135	2.80	12	0.11	0.11	0.08	0.08	...
627	9.53	0.48	0.55	6420	6386	82	3.07	6330	82	3.03	5	0.07	0.07	0.08	0.08	...
636	12.28	0.98	1.07	4660	4654	152	1.68	4636	152	1.64	12	0.12	0.12	0.07	0.07	...
676	12.86	1.04	1.10	4400	4507	34	0.61	4575	34	0.70	5	0.13	0.13	0.08	0.08	...
746	11.18	0.73	0.82	5280	5407	98	2.28	5288	98	2.15	18	0.15	0.15	0.13	0.13	...
879	12.67	1.03	1.14	4520	4531	152	1.50	4498	152	1.45	18	0.14	0.14	0.10	0.10	7.39 (1)
882	12.83	1.03	1.27	4500	4531	212	1.84	4282	210	1.50	25	0.18	0.18	0.15	0.16	0.58 (1)
883	12.93	1.04	1.24	4400	4507	46	0.75	4328	45	0.48	18	0.26	0.26	0.24	0.24	7.2 (7)
996	10.29	0.61	0.64	5880	5849	132	2.94	5939	133	3.03	12	0.10	0.10	0.08	0.09	...
1015	10.40	0.61	0.66	5860	5849	145	3.02	5858	145	3.03	12	0.10	0.10	0.08	0.08	...
1032	10.98	0.71	0.79	5400	5477	213	3.06	5385	212	2.95	18	0.15	0.14	0.12	0.12	1.31 (7)
1039	11.97	0.89	0.91	4720	4899	334	3.21	5023	335	3.38	18	0.17	0.16	0.12	0.13	...
1095	11.71	0.88	0.88	5000	4928	137	1.96	5107	139	2.19	12	0.12	0.11	0.07	0.07	...
1110	13.17	1.15	1.35	4240	4272	21	0.06	4173	20	-0.09	18	0.92	1.11	0.92	1.11	...
1122	9.17	0.42	0.50	6640	6655	67	3.12	6568	66	3.07	5	0.05	0.06	0.08	0.09	...
1124	12.20	0.94	1.02	4800	4760	217	2.19	4746	217	2.18	18	0.15	0.15	0.11	0.11	6.05 (1,6)
1132	9.30	0.46	0.54	6520	6474	46	2.81	6376	45	2.73	5	0.08	0.08	0.09	0.09	...
1139	9.25	0.44	0.49	6580	6564	51	2.93	6618	51	2.96	25	0.32	0.32	0.32	0.33	...
1200	9.82	0.50	0.62	6280	6300	67	2.88	6021	66	2.64	5	0.08	0.08	0.07	0.07	...
1207	10.395	0.605	0.655	5940	5868	141	3.02	5878	141	3.02	12	0.10	0.10	0.08	0.08	...
1215	10.415	0.59	0.65	5900	5928	125	2.97	5898	125	2.95	12	0.10	0.10	0.09	0.09	...
1275	11.33	0.79	0.81	5200	5206	159	2.42	5320	160	2.55	12	0.11	0.11	0.07	0.07	...
1309	9.34	0.43	0.50	6580	6609	42	2.85	6568	42	2.84	25	0.41	0.41	0.42	0.42	...
1332	12.41	0.98	1.05	4640	4654	35	0.82	4679	36	0.87	12	0.22	0.21	0.20	0.19	8.30 (1)
1454	12.74	1.04	1.18	4440	4507	86	1.07	4426	85	0.96	30	0.26	0.26	0.23	0.24	...
1514	10.385	0.62	0.66	5860	5810	161	3.08	5858	161	3.13	18	0.13	0.13	0.12	0.12	...
1531	13.46	1.23	1.41	4220	4128	99	0.67	4102	99	0.65	25	0.20	0.20	0.20	0.20	0.48 (1)
1593	11.03	0.73	0.77	5460	5407	163	2.67	5452	164	2.73	12	0.11	0.11	0.07	0.07	...
1613	9.75	0.50	0.58	6320	6300	103	3.15	6194	103	3.06	5	0.07	0.07	0.08	0.07	...
1653	13.38	1.17	1.44	4220	4233	109	0.86	4069	107	0.66	40	0.29	0.30	0.29	0.30	0.74 (7)
1776	10.79	0.685	0.745	5580	5567	140	2.71	5539	140	2.68	12	0.11	0.11	0.07	0.08	...
1794	10.28	0.58	0.62	5940	5967	55	2.49	6021	56	2.55	18	0.20	0.20	0.19	0.19	...
1797	10.01	0.52	0.60	6240	6214	125	3.22	6107	124	3.13	18	0.14	0.13	0.13	0.13	...
1856	9.89	0.52	0.57	6240	6214	85	2.95	6239	85	2.97	5	0.07	0.07	0.07	0.07	...
1883	12.54	0.99	1.17	4560	4629	250	2.23	4443	250	1.97	20	0.17	0.17	0.13	0.14	0.2354 (1)
1924	10.215	0.57	0.62	6020	6008	141	3.14	6021	141	3.16	18	0.13	0.13	0.12	0.12	...
2016	13.43	1.18	1.41	4220	4215	148	1.05	4102	147	0.92	18	0.13	0.12	0.12	0.13	...
2034	12.53	0.92	1.09	4760	4815	223	2.31	4595	221	2.00	30	0.21	0.21	0.18	0.18	0.55 (1)
2126	11.59	0.81	0.85	5120	5142	151	2.30	5196	151	2.36	12	0.11	0.11	0.07	0.07	...
2244	12.46	0.95	1.12	4720	4733	268	2.50	4536	266	2.21	30	0.23	0.23	0.21	0.20	0.57 (2)
2311	11.23	0.78	0.79	5240	5239	141	2.36	5385	142	2.53	12	0.11	0.11	0.07	0.07	...
2341	10.77	0.68	0.695	5620	5585	140	2.73	5722	141	2.87	12	0.11	0.10	0.08	0.08	8.2 (6)
2366	11.37	0.78	0.80	5240	5239	189	2.63	5352	190	2.77	12	0.11	0.12	0.07	0.08	...
2462	11.37	0.80	0.80	5200	5174	103	2.05	5352	104	2.26	12	0.12	0.12	0.08	0.08	...
2506	10.15	0.56	0.64	6080	6048	108	2.97	5939	107	2.87	18	0.14	0.14	0.13	0.13	...
2588	13.24	1.14	1.33	4300	4291	78	0.72	4199	77	0.60	18	0.17	0.17	0.15	0.16	...
2644	10.95	0.71	0.74	5520	5477	186	2.89	5557	186	2.98	12	0.11	0.11	0.08	0.08	...
2741	12.53	0.97	1.08	4680	4680	91	1.35	4616	90	1.26	30	0.25	0.25	0.23	0.23	5.. (5)
2786	10.17	0.57	0.63	6040	6008	128	3.06	5980	127	3.03	18	0.13	0.13	0.12	0.12	2.21 (7)
2870	12.39	0.97	1.06	4680	4680	69	1.19	4658	68	1.16	12	0.14	0.14	0.10	0.10	...
3019	13.41	1.17	1.39	4220	4233	52	0.43	4125	50	0.28	30	0.42	0.43	0.41	0.43	...
3063	13.42	1.13	1.42	4300	4311	139	1.13	4091	137	0.85	25	0.17	0.16	0.15	0.16	0.89 (6)
3163	12.65	0.97	1.17	4700	4680	222	2.11	4443	220	1.77	30	0.21	0.21	0.18	0.18	10.08 (1)
3179	9.93	0.53	0.62	6180	6172	121	3.16	6021	121	3.03	12	0.10	0.10	0.09	0.09	...
3187	13.03	1.12	1.28													

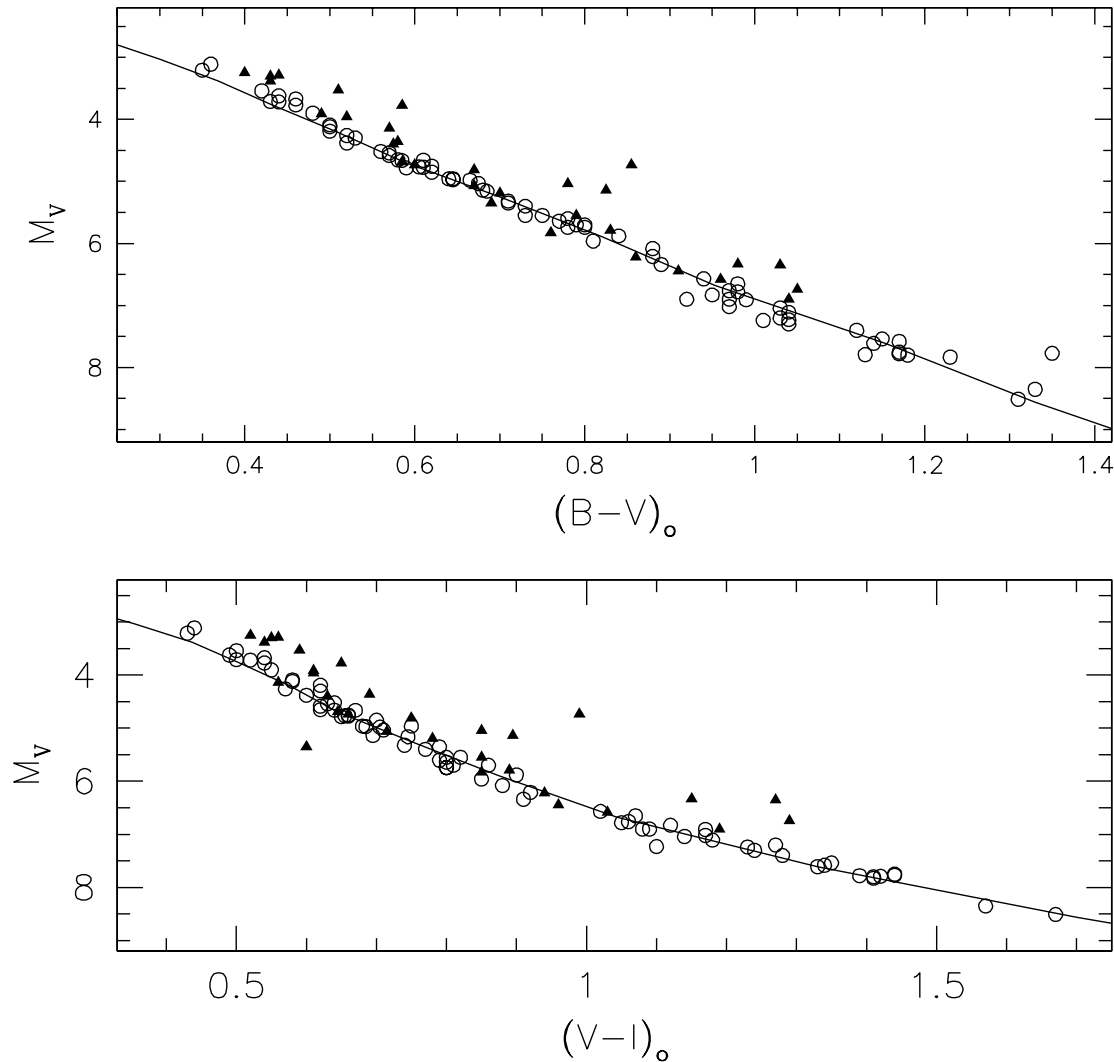


Fig. 1. The color magnitude diagrams of our final non-binary Pleiades L sample (open circles) and stars rejected as binaries (filled triangles). The Pleiades data is plotted assuming a distance modulus of 5.63 and with a 100 Myr isochrone from Pinsonneault et al. (1998).

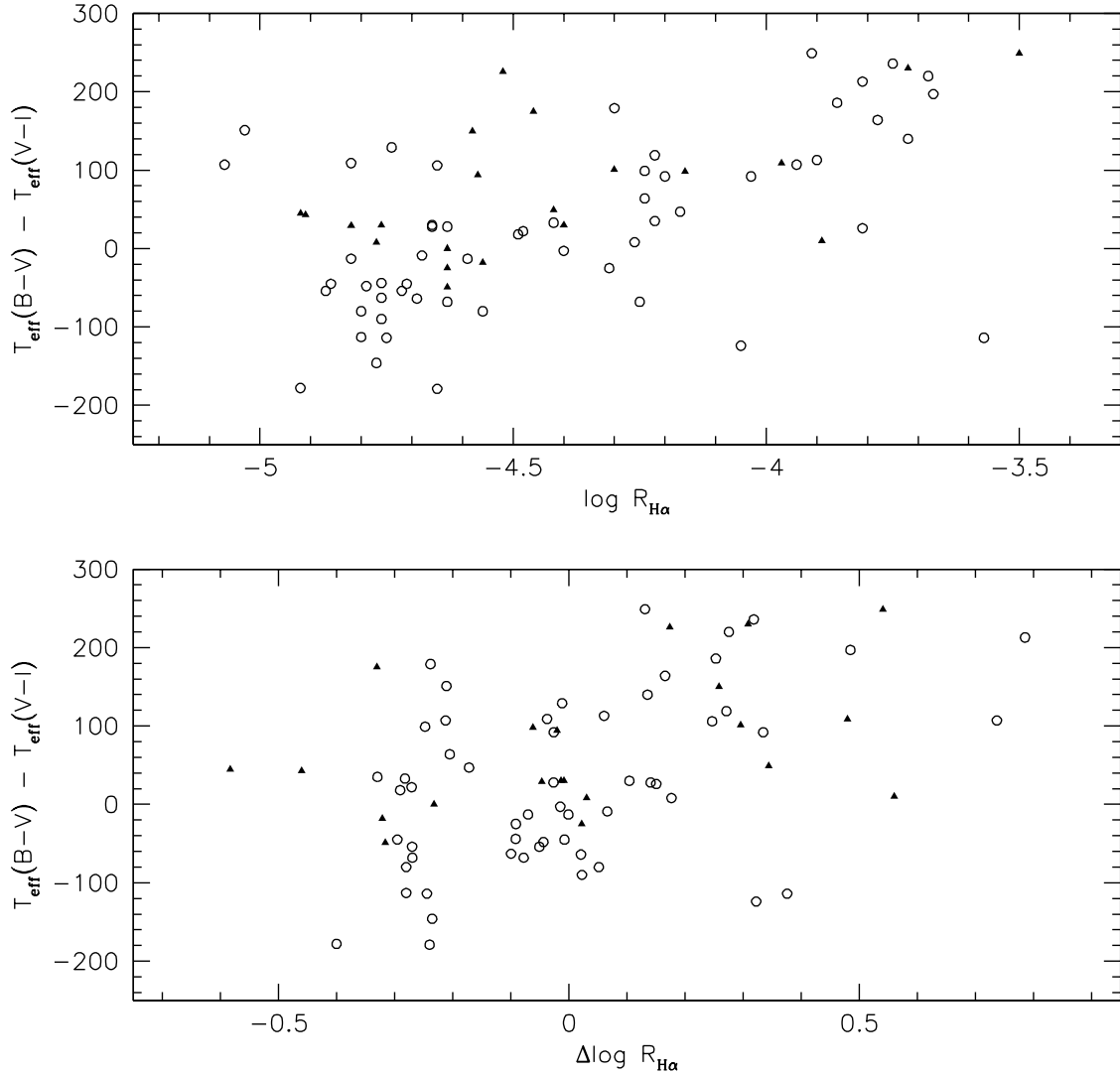


Fig. 2. The top panel shows the difference between our $(\text{B}-\text{V})$ - and $(\text{V}-\text{I})$ -based T_{eff} estimates versus $\text{H}\alpha$ flux ratio (relative to the stellar bolometric flux) from Soderblom et al. (1993). The bottom panel shows the temperature difference versus the residual $\text{H}\alpha$ flux ratio, which is the flux ratio less a fitted color dependency.

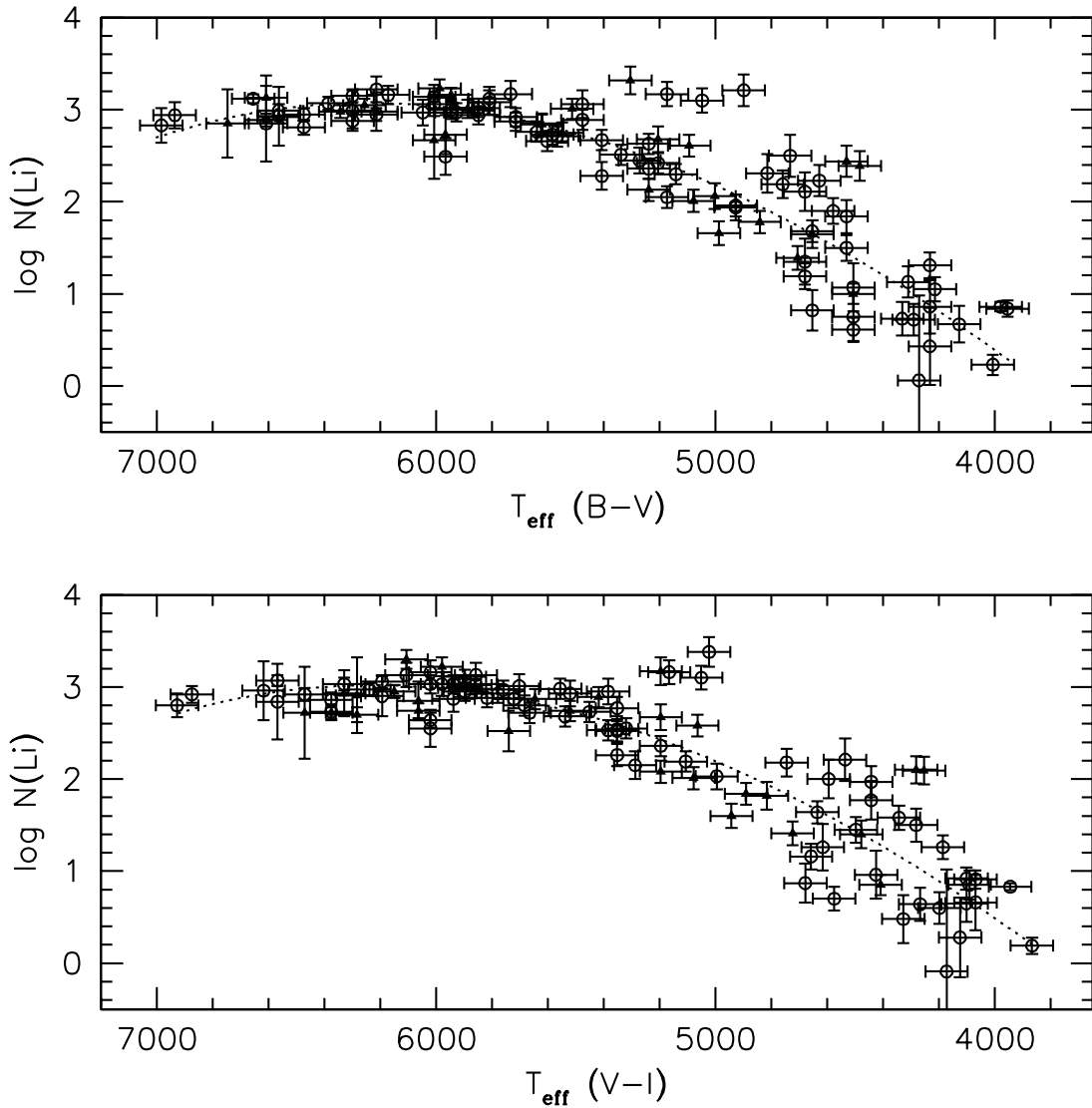


Fig. 3.1 Liabundances (with derived errors) vs. T_{eff} from our $(B-V)$ measures (top) and $(V-I)$ measures. The well-known declining trend of Liabundance with decreasing T_{eff} is fitted with a fourth order Legendre polynomial (dashed line).

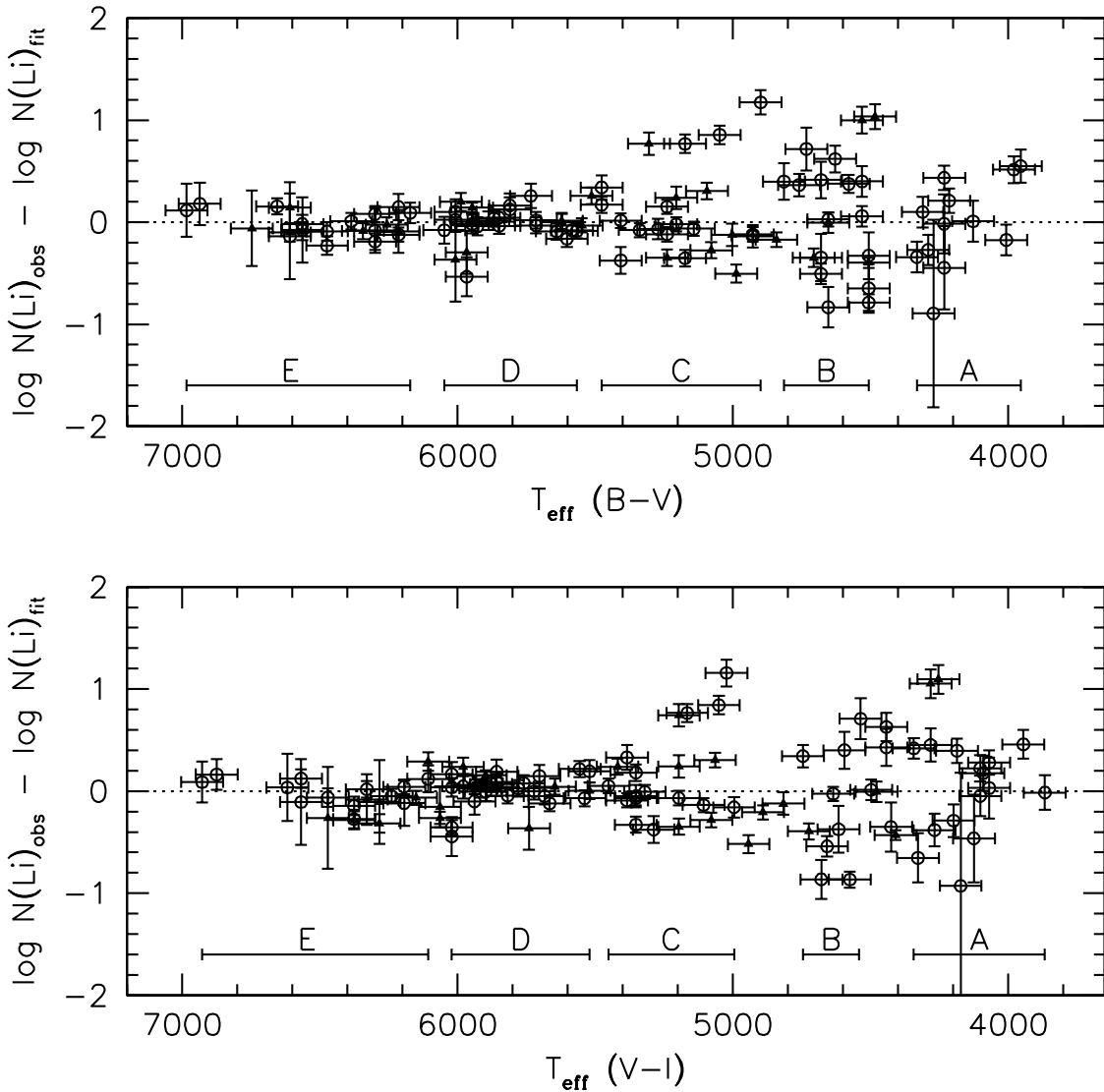


Fig. 4.1 Same as Figure 3 except the differential (detrended) Li abundances and related errors are shown. Temperature bins used in considering the scatter of Li abundances as a function of T_{eff} are labeled in both plots.

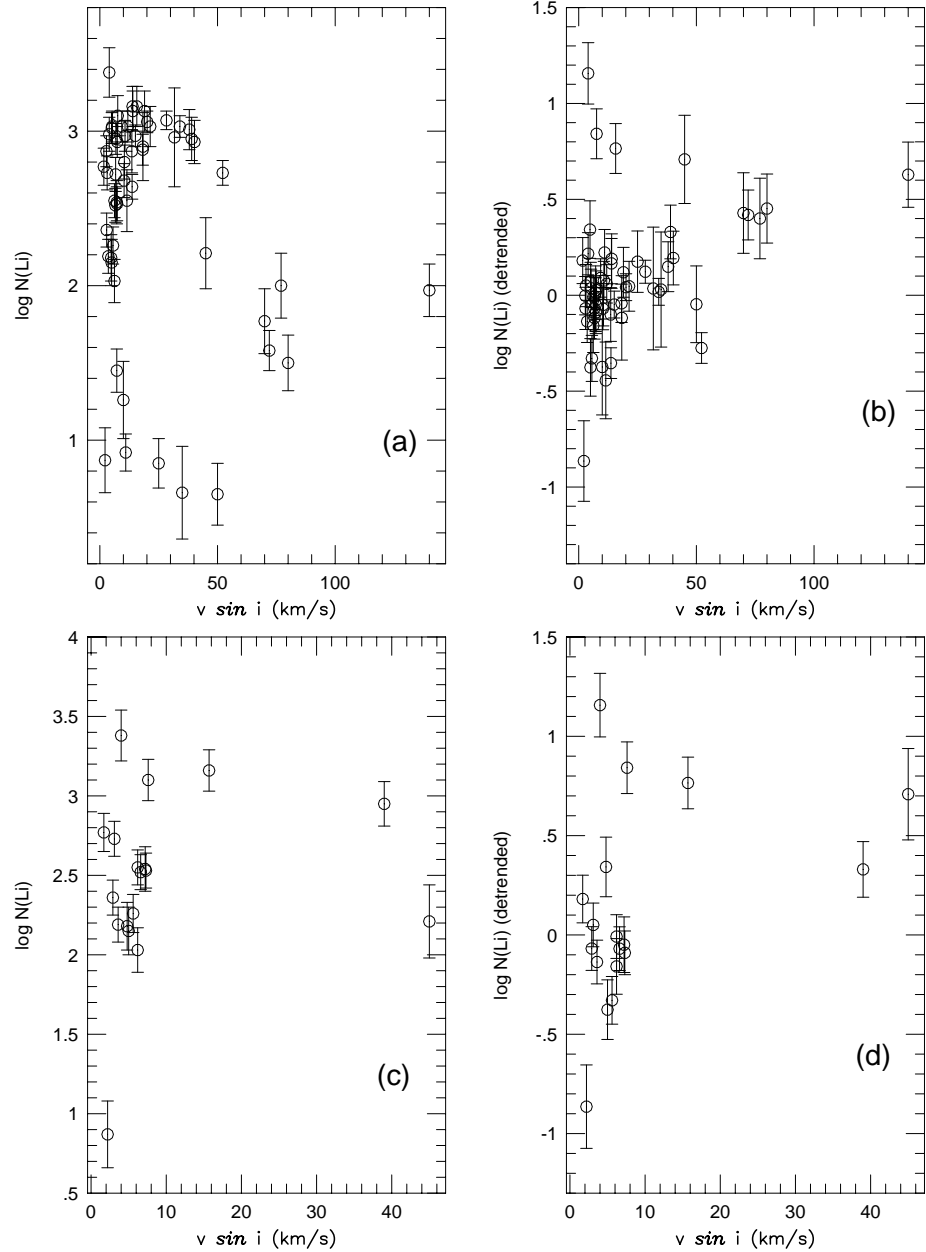


Fig. 5. Projected rotational velocity $v \sin i$ versus $(V - I)$ -based Li results for (a) all T_e and absolute Li abundance (b) all T_e and differential detrended Li abundance (c) $T_e = 4500 - 5500$ K and absolute Li abundance (d) $T_e = 4500 - 5500$ K and differential Li abundance.

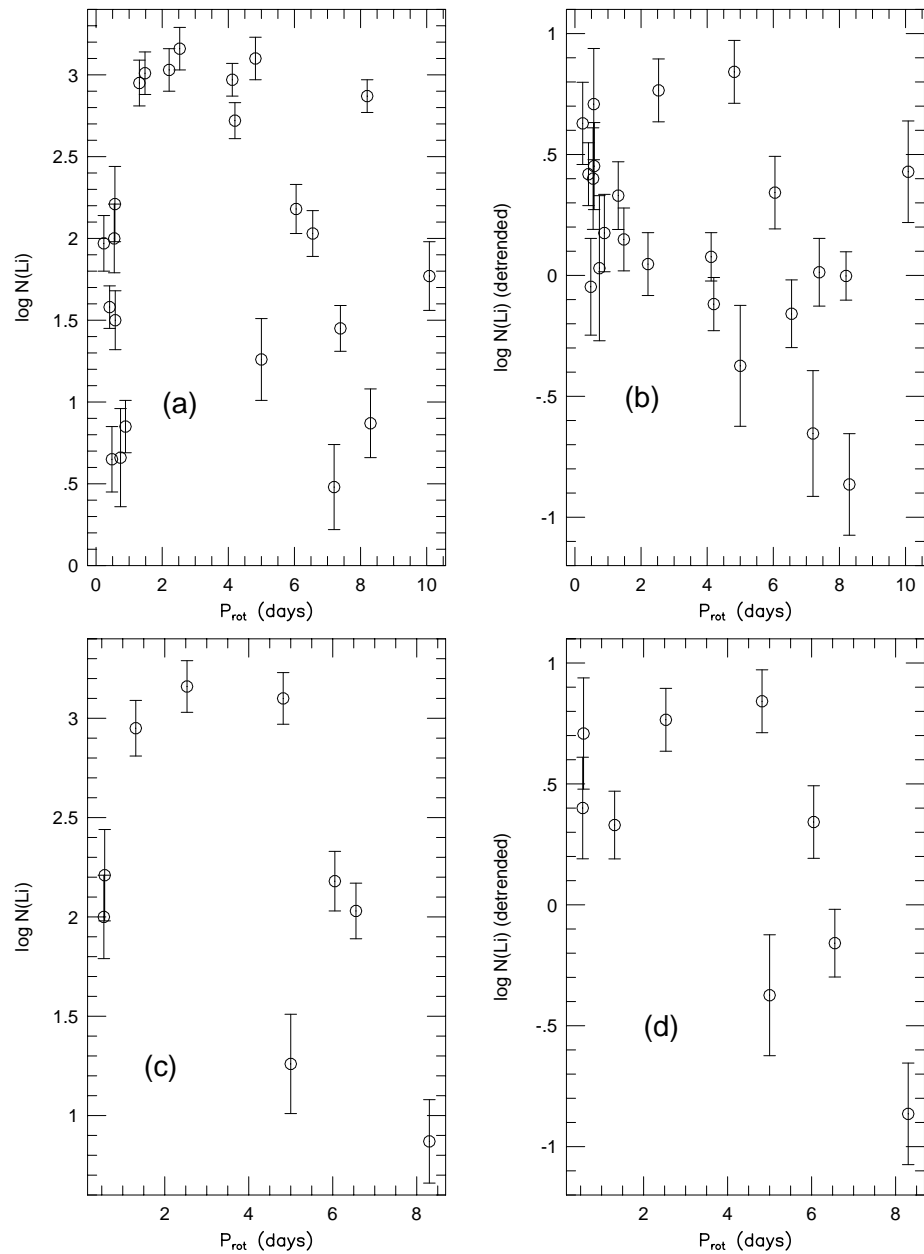


Fig. 6. Same as Figure 5 except rotational period, P_{rot} , in days is plotted instead of $v \sin i$.

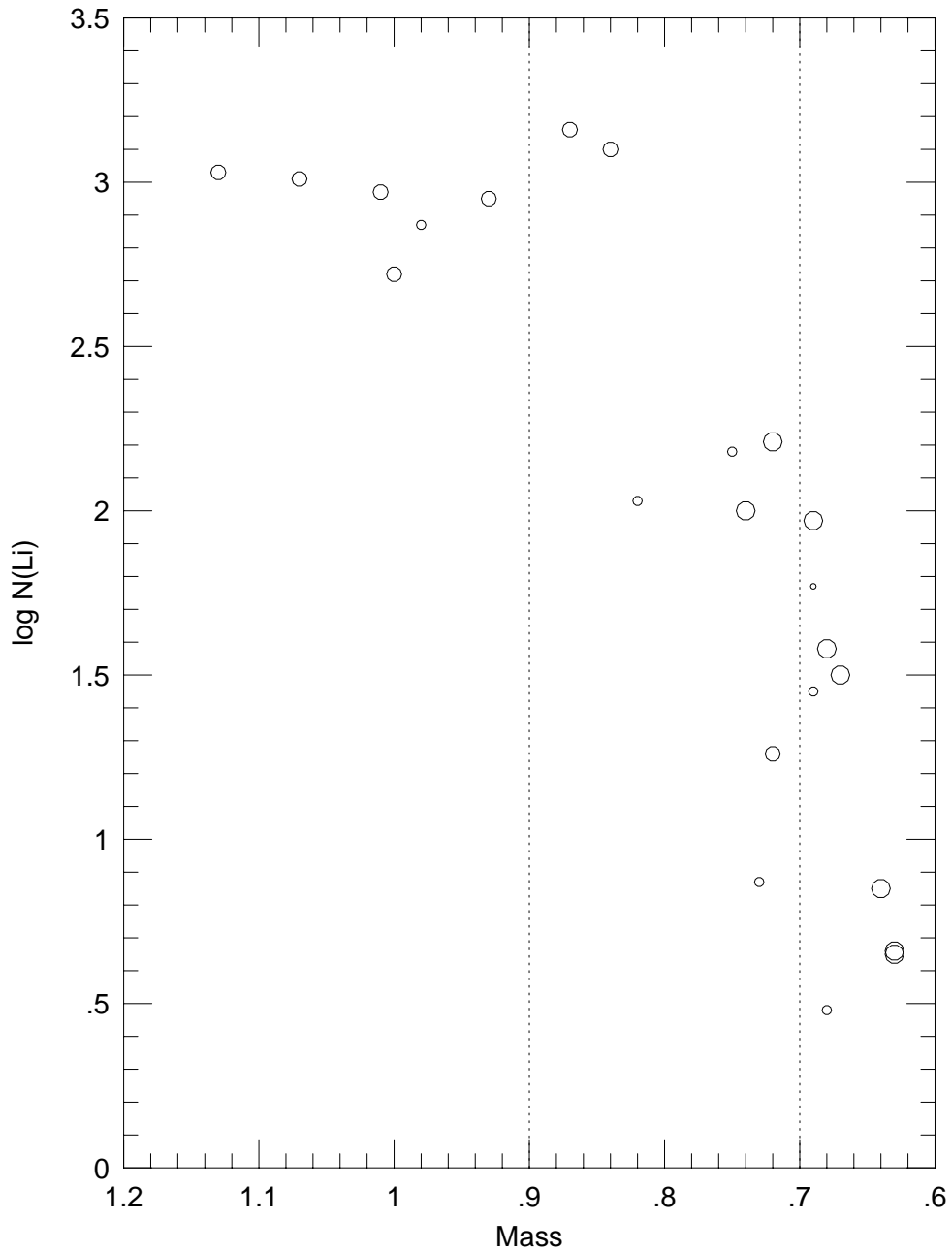


Fig. 7. Our $(V - I)$ -based Li abundances versus stellar mass. The symbol size corresponds to rotational period. The largest circles represent stars with $P_{\text{rot}} < 1$ d, the medium sized circles represent those with P_{rot} between 1 d and 5 d, while the smaller circles indicate stars with P_{rot} between 5 d and 10 d. The tiny circle denotes a star with $P_{\text{rot}} > 10$ d. The dashed lines denote the mass range $M = 0.7 - 0.9 M_{\odot}$.

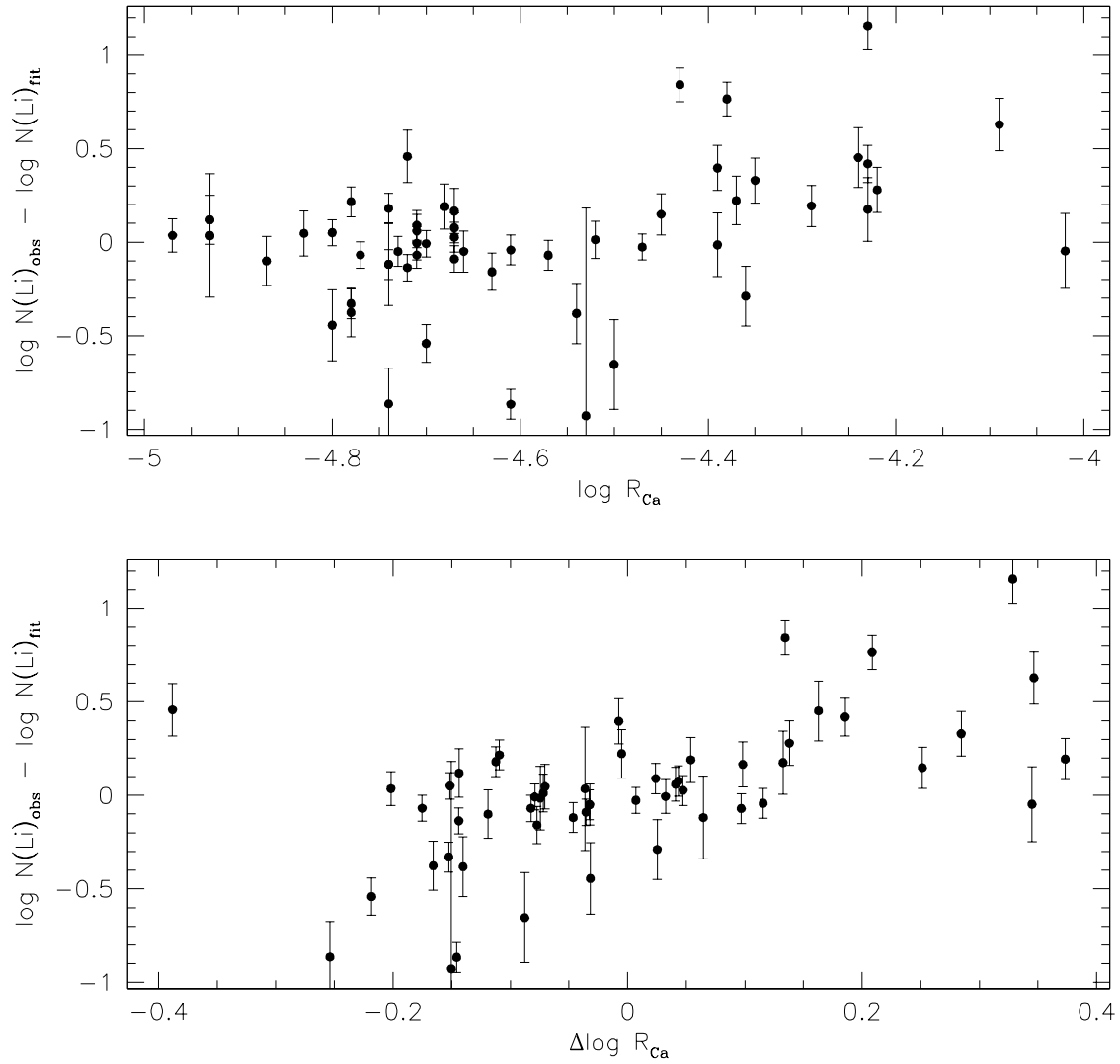


Fig. 8. Our (V - I)-based differential Li abundances are plotted versus the Ca II infrared triplet flux ratio (top panel) and residual flux ratio (bottom), which is the flux ratio less a fitted color dependency.

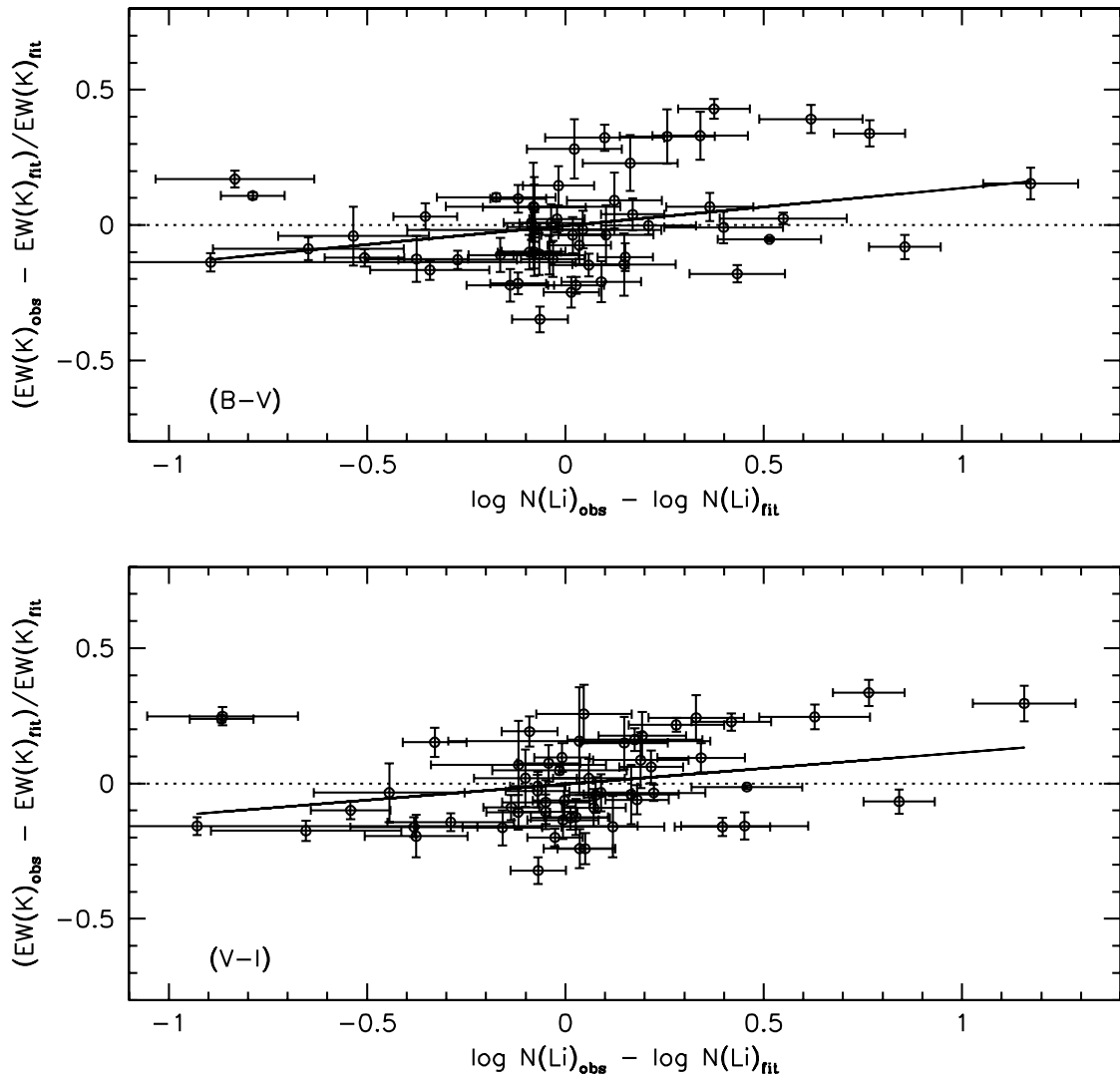


Fig. 9. | Differential 7699 K K equivalent widths ([observed - fitted]/ fitted) versus our (B - V)-based (top panel) and (V - I)-based differential Li abundances (bottom panel).

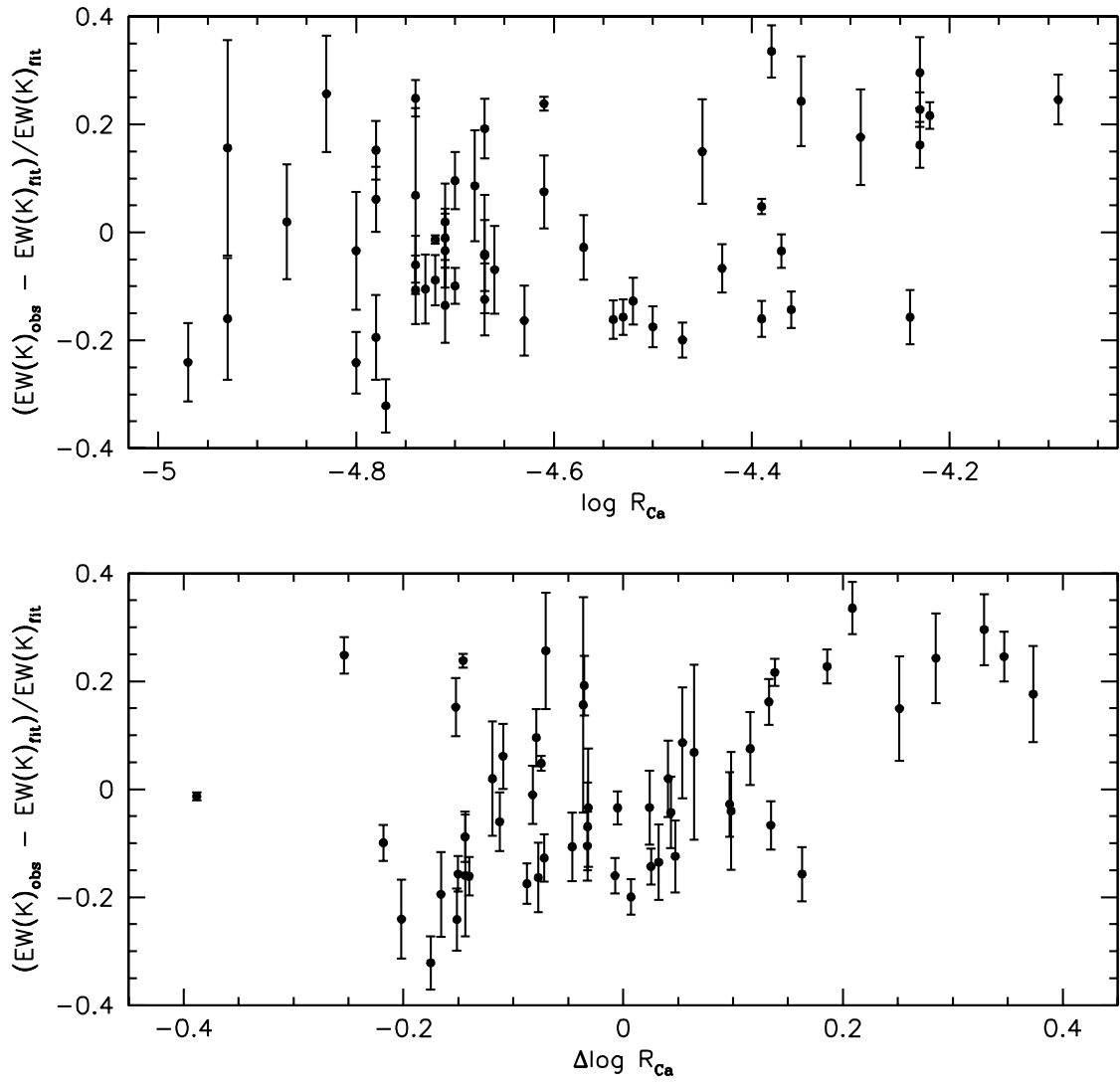


Fig. 10. The (V - I)-based differential K I line strengths are plotted versus the Ca II infrared triplet flux ratio (top panel) and residual flux ratio (bottom panel).

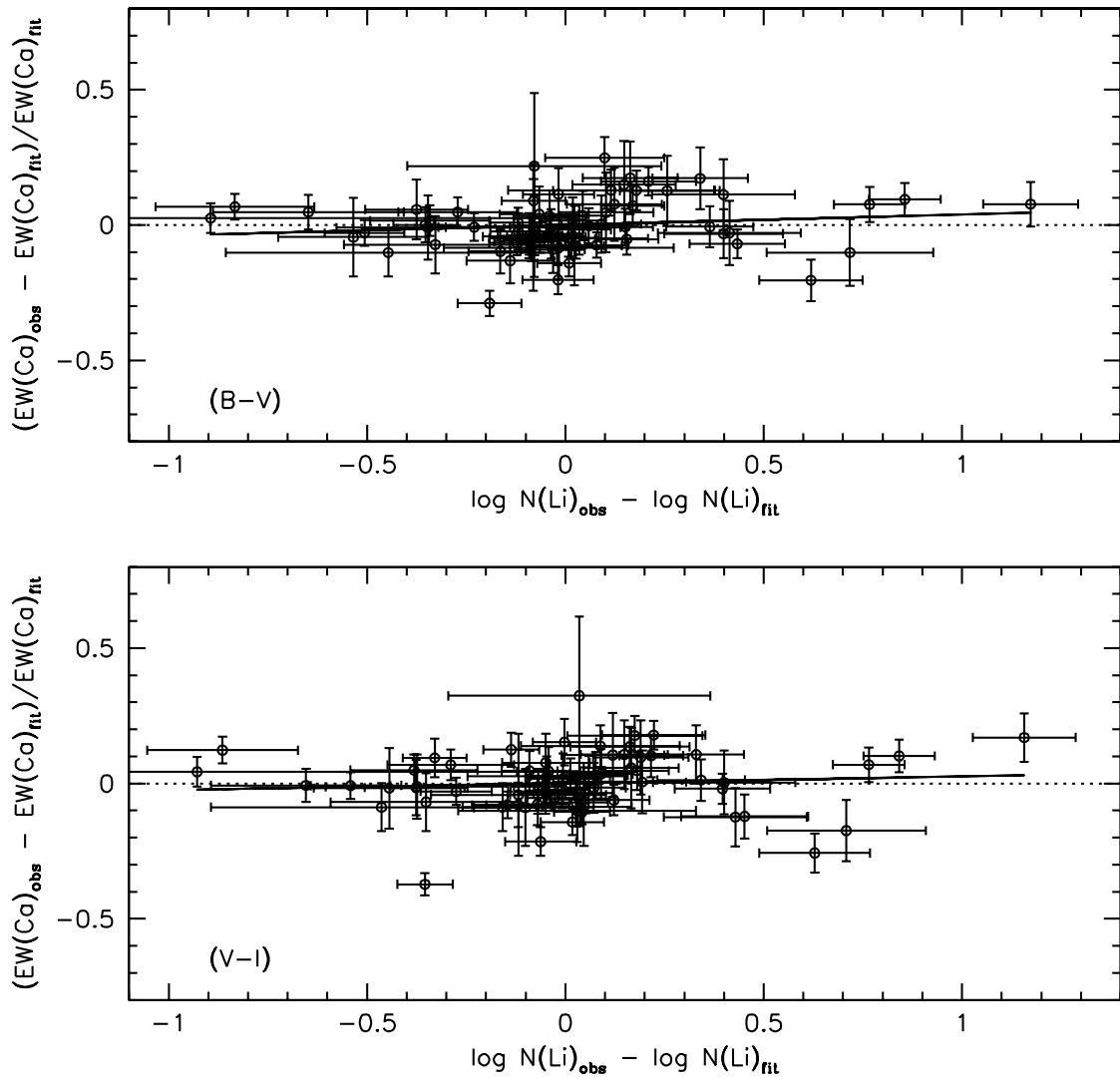


Fig. 11. | Differential 6717 Ca I equivalent widths versus our $(B - V)$ -based (top panel) and $(V - I)$ -based (bottom panel) differential Li abundances.